nature medicine

Thalidomide stimulates vessel maturation and reduces epistaxis in individuals with hereditary hemorrhagic telangiectasia

Franck Lebrin[1], Samly Srun[1], Karine Raymond[2], Sabrina Martin[1], Stieneke van den Brink[3], Catarina Freitas[1], Christiane Bréant[1], Thomas Mathivet[1], Bruno Larrivée[1], Jean-Léon Thomas[4], Helen M Arthur[5], Cornelis J J Westermann[6], Frans Disch[6], Johannes J Mager[6], Repke J Snijder[6], Anne Eichmann[1,8] & Christine L Mummery[7,8]

Hereditary hemorrhagic telangiectasia (HHT) is an inherited disorder characterized by vascular malformations. Many affected individuals develop recurrent nosebleeds, which can severely affect their quality of life and are clinically difficult to treat. We report here that treatment with thalidomide reduced the severity and frequency of nosebleeds (epistaxis) in the majority of a small group of subjects with HHT tested. The blood hemoglobin levels of the treated individuals rose as a result of reduced hemorrhage and enhanced blood vessel stabilization. In mice heterozygous for a null mutation in the *Eng* gene (encoding endoglin), an experimental model of HHT, thalidomide treatment stimulated mural cell coverage and thus rescued vessel wall defects. Thalidomide treatment increased platelet-derived growth factor-B (PDGF-B) expression in endothelial cells and stimulated mural cell activation. The effects of thalidomide treatment were partially reversed by pharmacological or genetic interference with PDGF signaling from endothelial cells to pericytes. Biopsies of nasal epithelium from individuals with HHT treated or not with thalidomide showed that similar mechanisms may explain the effects of thalidomide treatment in humans. Our findings demonstrate the ability of thalidomide to induce vessel maturation, which may be useful as a therapeutic strategy for the treatment of vascular malformations.

HHT is an autosomal dominant vascular disease with a prevalence of about 1 in 10,000 individuals. It is caused by mutations in either the *ENG* gene or the gene encoding activin receptor-like kinase-1 (ALK-1) (*ACVRL1*). These genes encode receptors for members of the transforming growth factor-β (TGF-β) family of ligands[1,2]. These receptors are expressed primarily by endothelial cells and signal to the same downstream Smad proteins, second messengers that translocate to the nucleus after activation[3,4]. Clinical manifestations of HHT include arteriovenous malformations (AVMs), which range from small telangiectases (regions of capillary dilatation) in the nasal septum, oral mucosa and gastrointestinal tract to large AVMs in the lung, brain and liver. Large AVMs consist of direct connections between arterioles and venules without intervening capillaries; these can cause severe complications if not recognized and treated. Telangiectasic lesions are characterized by not only dilation of the vascular lumen but also thinning of the vascular wall. Such lesions can cause chronic nasal and gastrointestinal hemorrhages that result in intense bleeding and severe anemia. Multiple lesions disseminated over the entire mucosal surface are common in affected individuals, making local treatment difficult. To limit blood loss, the few therapeutic options used include manipulation of the coagulation and fibrolytic pathways, surgical replacement of nasal epithelium with skin, or topical application of anti-inflammatory drugs. However, these options offer, at best, limited hemorrhage-free intervals and all have side effects[5].

The development of vascular malformations in individuals with HHT has been attributed to decreased TGF-β activation and increased vascular endothelial growth factor (VEGF) production[6–8]. Deregulation of these key angiogenic factors is thought to lead to abnormal endothelial cell proliferation and migration and to extracellular matrix production and degradation, resulting in disengagement of the endothelium from the surrounding mural cells. These abnormalities cause vessels to weaken and become prone to bleeding, a major feature of HHT that increases in frequency with age[4,9]. Inhibitors of angiogenesis could therefore be beneficial in treating symptoms resulting from these vascular anomalies in affected individuals[10]. However, antiangiogenic drugs may also affect normal

[1]Institut National de la Santé et de la Recherche Médicale U833, Collège de France, Paris, France. [2]Institut Curie, Centre de Recherche, Centre National de la Recherche Scientifique UMR144, Paris, France. [3]Hubrecht Institute, Developmental Biology and Stem Cell Research, Utrecht, The Netherlands. [4]Institut National de la Santé et de la Recherche Médicale U711, Paris, France. [5]Institute of Human Genetics, International Centre for Life, Newcastle University, Newcastle, UK. [6]St. Antonius Hospital, Nieuwegein, The Netherlands. [7]Department of Anatomy and Embryology, Leiden University Medical Centre, Leiden, The Netherlands. [8]These authors contributed equally to this work. Correspondence should be addressed to F.L. (franck.lebrin@college-de-france.fr) or C.L.M. (c.l.mummery@lumc.nl).

Received 18 September 2009; accepted 8 March 2010; published online 4 April 2010; doi:10.1038/nm.2131

Table 1 Clinical characteristics of subjects with HHT after treatment with thalidomide.

	Nosebleeds						Number of blood transfusions		Median hemoglobin concentration		
	1 month before thalidomide			After 3 months of thalidomide			Year before	Year after	12 months before	During thalidomide	12 months after
Subject	Severity of bleeding	Number per week	Duration (min)	Severity of bleeding	Number per week	Duration (min)			(mmol ml^{-1})	(mmol ml^{-1})	(mmol ml^{-1})
1	**	32	NA	*	11	NA	1	0	5.75	6.2	NA
2	**	32	25–30	*	2	<5	6	0	6.70	8.6§	7.4
3	**	35	15–20	**	35	5–15	NA	NA	5.45	6.55§	5.6
4	***	21	15–20	*	14	10	0	0	6.70	7.85§	7.4
5	**	35	NA	*	3	NA	NA	NA	NA	NA	NA
6	**	18	NA	**	1	NA	0	0	6.6	8.7§	8
7#	***	26	20–25	**	20	15–20	0	0	5.1	6.9§	6.5
8#	***	NA	20–60				3		4.75		
9#	**	28	30				NA		7.20		
10#	***	59	10–90				8		4.3		

We treated subjects 1–7 with thalidomide; subjects 8–10 were untreated controls.
# indicates the subjects in **Figure 4c**. *, mild; **, moderate; ***, severe. NA, not available. §$P < 0.05$ for comparisons of values before and during thalidomide treatment.

physiological processes, and bevacizumab, an antibody that targets VEGF, has been reported to both cause[11] and reduce epistaxis[12]. Off-label drug use of this agent in individuals with HHT may reduce disease symptoms but may also affect normal physiology, and therefore requires cautious clinical implementation and preferably a well-described mechanism of action.

Thalidomide, originally used to treat nausea in pregnancy in the early 1960s, was removed from the market when severe congenital defects became evident in newborns, a result of antiangiogenic activity that reduced the blood supply to fetal organs and tissues at specific times of development[13,14]. These defects occurred when drug exposure took place within a short, time-sensitive window between day 20 and day 36 of gestation. Just one 100-mg tablet of thalidomide was enough to cause limb defects[13,14]. However, thalidomide has enjoyed a renaissance in recent years. Under strict guidelines and carefully controlled inclusion criteria, it is now used to treat various pathologies: it reportedly inhibits bleeding in individuals with certain gastrointestinal diseases[10,15–17] and in HHT patients who received thalidomide as an antiangiogenic cancer therapy[18,19]. The mechanisms by which thalidomide inhibits bleeding from vascular malformations are unknown, although it has been reported to regulate expression of components of signaling pathways that are involved in stimulating or inhibiting angiogenesis, such as the VEGF pathway[20]. More recently, it has been shown to target endothelial tip cells of immature vessels[14].

Here we have examined the effects of thalidomide on subjects with HHT, specifically monitoring effects on the severity of nosebleeding (epistaxis). We have also investigated the mechanisms by which thalidomide affects angiogenesis and vessel remodeling to explore in more depth the possibility that thalidomide may have a broader therapeutic utility for treating vascular malformations.

RESULTS

Thalidomide lowers nosebleed frequency in subjects with HHT

We treated seven subjects with HHT with severe and recurrent epistaxis with thalidomide. The dose given was comparable to that prescribed in the 1960s to treat nausea in pregnancy[13]. The subjects with HHT were between 48- and 75- years-old and had mutations in either *ENG* or *ACVRL1* (**Table 1** and **Supplementary Fig. 1**). Oral administration of 100 mg of thalidomide daily significantly ($P \leq 0.05$) lowered the frequency of epistaxis in six of the seven subjects and its duration in three of the four subjects for whom data were available, all within 1 month of administration of the first dose (**Table 1**). The average hemoglobin concentration in peripheral blood increased without additional dietary iron supplementation in five out of six subjects in whom iron supplementation was recorded (**Table 1** and **Supplementary Fig. 1**). Before treatment, four individuals who suffered from 18–32 nosebleeds per week required between one and six blood transfusions yearly to prevent anemia. These four subjects did not require additional blood transfusions after being treated with thalidomide in a 6-month to 5-year follow-up (**Table 1**). Six out of the seven subjects treated showed only minor side effects: mild constipation, loss of libido, drowsiness and lethargy; the remaining subject stopped treatment 19 months after the first dose because of peripheral neuropathy (data not shown). In this individual and in two others who stopped treatment for reasons unrelated to side effects, epistaxis returned after treatment cessation. Hemoglobin concentrations for two of the subjects dropped significantly ($P \leq 0.05$) to pretreatment levels (**Table 1** and **Supplementary Fig. 1**); for the third, the drop was substantial, but too few hemoglobin-concentration values were available to allow statistical analysis.

Control subjects with HHT but not treated with thalidomide consistently had lower hemoglobin concentrations than both the normal physiological range and the treated subjects (**Table 1** and **Supplementary Fig. 1**). These data indicate that thalidomide might be a therapeutic option for subjects with HHT and severe epistaxis for whom other treatments have failed.

Thalidomide promotes vessel maturation

To investigate how thalidomide might cause antihemorrhagic effects in the treated subjects, we examined its effects in several angiogenesis models. We first used spheroids of differentiating mouse embryonic stem cells (embryoid bodies). When plated onto collagen I in the presence of VEGF and basic fibroblast growth factor, embryoid bodies undergo sprouting angiogenesis[21]. We tested the effects of adding various concentrations of thalidomide in this model. After allowing the embryoid bodies to undergo angiogenesis for a period of 3 d, we fixed and stained them for platelet–endothelial cell adhesion molecule-1 (PECAM-1) as an endothelial cell marker, and we then quantified the number of vessel sprouts formed. At very high doses (100 μg ml^{-1}) that reached the solubility threshold and verged on being cytotoxic, thalidomide inhibited vessel formation; however, at lower concentrations (10–50

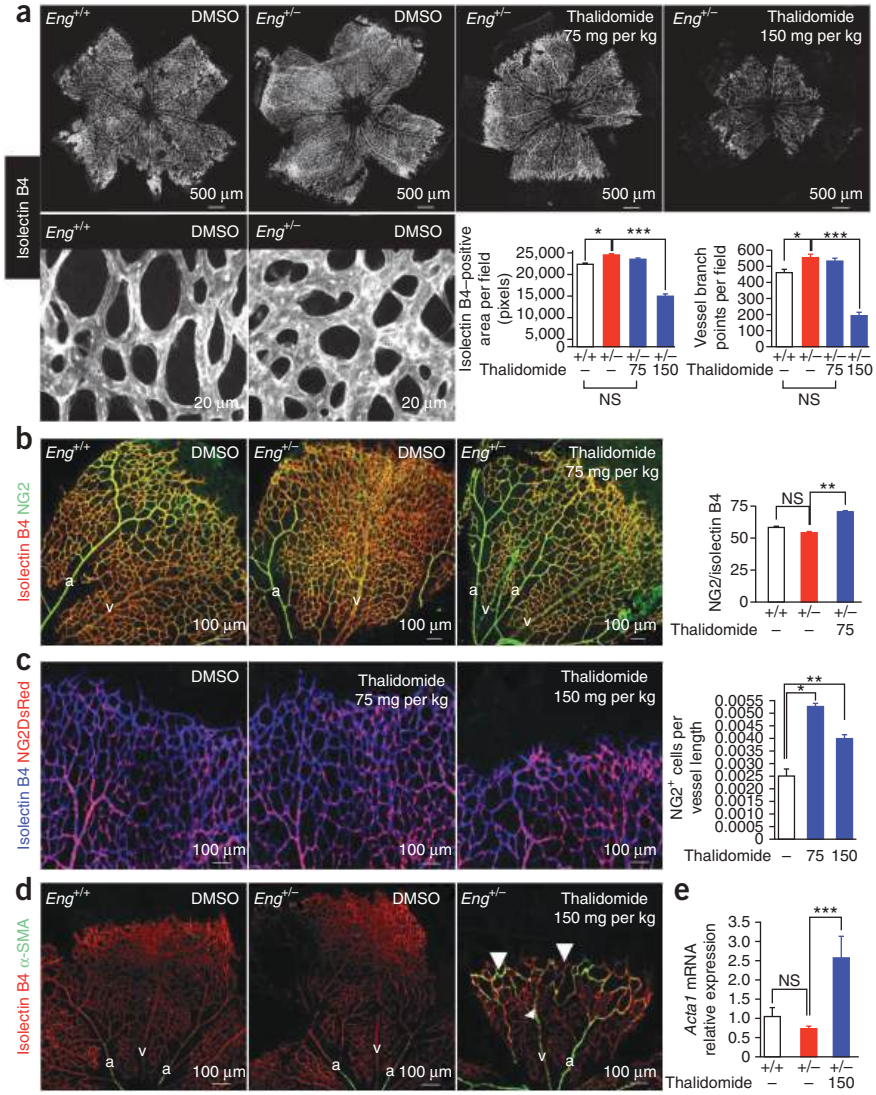

Figure 1 Thalidomide normalizes excessive vessel branching in the retina of *Eng*$^{+/-}$ mice and enhances pericyte/VSMC coverage. (**a**) Top, isolectin B4–stained endothelial cells in retinal vessels in *Eng*$^{+/+}$ (WT) ($n = 14$) and *Eng*$^{+/-}$ mice ($n = 13$) at P7 after intraperitoneal injection with DMSO (carrier control) or 75 mg per kg body weight ($n = 15$) or 150 mg per kg body weight ($n = 6$) thalidomide at P4. At bottom left are higher magnifications of the vascular front in *Eng*$^{+/+}$ and *Eng*$^{+/-}$ mice from the images in the top row. Bottom right, quantification of isolectin B4–positive surface area density and number of vessel branch points per field. (**b**) Left, confocal images of flat-mounted retinas labeled with antibody specific for isolectin B4 (red, marking endothelial cells) and antibody specific for NG2 (green, marking pericytes) from wild-type ($n = 14$) and *Eng*$^{+/-}$ mice ($n = 13$) at P7 after intraperitoneal injection of DMSO or 75 mg per kg body weight thalidomide ($n = 15$). Right, the ratio of total area of NG2-positive pericytes to isolectin B4–positive capillaries. (**c**) Left, confocal images of retinas from NG2DsRedBAC-transgenic mice at P7 injected intraperitoneally at P4 with DMSO (carrier control) ($n = 4$), thalidomide at 75 mg per kg body weight ($n = 4$) or thalidomide at 150 mg per kg body weight ($n = 7$) and stained with isolectin B4 to reveal the vascular plexus. Right, quantification of the number of pericytes per isolectin-B4 surface area. (**d**) Left, isolectin B4–specific (red) staining of endothelial cells and α-SMA–specific (green) staining of vascular smooth muscle cells in whole-mount retinas of *Eng*$^{+/+}$ ($n = 6$) and *Eng*$^{+/-}$ ($n = 13$) mice treated at P4 with DMSO (carrier control) or 150 mg per kg body weight thalidomide ($n = 6$) and analyzed at P7. VSMC coverage of veins is indicated by the white arrow, and the vascular front is indicated by white arrowheads. (**e**) Quantification of *Acta1* expression in retinas. All error bars represent s.e.m. $^*P < 0.05$, $^{**}P < 0.01$ and $^{***}P < 0.001$, results from unpaired *t* test. NS, not significant; a, arteries; v, veins.

μg ml^{-1}), thalidomide enhanced endothelial sprouting compared to DMSO (vehicle control)-treated cultures (**Supplementary Fig. 2a**,**b**). The general architecture of the vessel sprouts was unchanged by thalidomide treatment, with branches composed of stalk cells guided by tip cells that occasionally fused to adjacent vessels to form a network (**Supplementary Fig. 2a**). Notably, thalidomide at a low concentration (25 μg ml^{-1}) stimulated the recruitment of mural cells to the vessel branches. Under control conditions, only a small proportion of the endothelial cell sprouts was surrounded by α-smooth muscle actin (α-SMA)-positive cells (vascular smooth muscle cells (VSMCs)). Thalidomide increased the proportion of endothelial sprouts covered by α-SMA$^+$ cells compared to control (DMSO-treated) cultures (**Supplementary Fig. 3**). These results suggest that the antihemorrhagic properties of thalidomide in individuals with HHT might be the result of direct inhibition of endothelial cell proliferation and migration[13,14] as well as of increased mural cell coverage; such coverage might stabilize blood vessels and prevent bleeding caused by rupture of the vascular malformations in these individuals.

To explore the possibility that thalidomide promotes vessel maturation *in vivo*, we took advantage of *Eng*$^{+/-}$ mutant mice that develop age-dependent vascular lesions similar to those seen in individuals with HHT[22,23]. We first focused on the neonatal retina, a vascular bed that is amenable to testing the effects of agents that modulate angiogenesis[24]. As in wild-type littermates, postnatal day 7 (P7) *Eng*$^{+/-}$ mice showed morphologically distinguishable arteries and veins in the retina, and endothelial tip cells formed filopodial protrusions at the sprouting front of the plexus (**Fig. 1a**). However, *Eng*$^{+/-}$ retinas showed excessive angiogenesis, with a denser, more highly branched vascular plexus compared to wild-type littermates (**Fig. 1a**). A low dose of thalidomide (75 mg per kg body weight) administered once at P4 was sufficient to normalize the inappropriate and excessive vessel sprouting in retinas of P7 *Eng*$^{+/-}$ mice (**Fig. 1a**). A higher dose of thalidomide (150 mg per kg body weight) retarded growth, as evidenced by the lower weight of the *Eng*$^{+/-}$ pups treated at this dose compared to untreated littermates or pups treated with lower doses (**Supplementary Fig. 4**), and markedly reduced angiogenesis in *Eng*$^{+/-}$ mice (**Fig. 1a**). Thus, thalidomide had a dose-dependent effect on retinal angiogenesis, with high concentrations required to reduce vessel sprouting, similar to the effects of thalidomide seen on embryoid bodies. Mural cell coverage appeared normal in retinas of P7 *Eng*$^{+/-}$ mice compared to wild-type littermates, as revealed by staining for chondroitin sulfate proteoglycan NG2, which marks VSMCs and pericytes (**Fig. 1b**). However, even at a low dose (75 mg per kg body weight), thalidomide

stimulated pericyte recruitment to the vasculature, as assessed by measuring the ratio of NG2 to isolectin B4 labeling (**Fig. 1b**).

We next used NG2DsRedBAC-transgenic mice, which express the red fluorescent protein (DsRed) under the control of the *Cspg4* (encoding NG2) promoter[25], to quantify the number of pericytes in the retina. DsRed$^+$ cells were distributed widely throughout the vascular plexus in close apposition to endothelial cells, covering the arteries completely and the veins partially (**Fig. 1c**). We also found solitary DsRed$^+$ cells at capillary branch points (**Fig. 1c**). Thalidomide treatment at both doses (75 and 150 mg per kg body weight) strongly stimulated pericyte recruitment to the vascular plexus of P7 NG2DsRedBAC-transgenic mice (**Fig. 1c**). In addition, the proportion of pericytes expressing Ki67, a marker of cycling cells, increased significantly ($P \leq 0.01$), indicating that thalidomide induced cell cycle entry of pericytes (**Supplementary Fig. 5**). Higher doses of thalidomide resulted in an extension of VSMC coverage to the veins and to the vascular front (**Fig. 1d**) and also resulted in an increased expression of *Acta1* (encoding α-actin-1) messenger RNA (**Fig. 1e**). Thus, thalidomide treatment of postnatal mice *in vivo* promotes retinal vessel maturation by enhancing pericyte and VSMC coverage.

Thalidomide-induced mural cell recruitment requires PDGF-B

To investigate possible mechanisms of thalidomide action, we measured mRNA expression of growth factors and receptors regulating angiogenesis and mural cell recruitment in P7 retinal mRNA extracted from thalidomide-treated and untreated *Eng*$^{+/-}$ and wild-type littermates. Thalidomide injection did not affect mRNA expression of *Vegfa* (**Fig. 2a**) or its receptors *Flt1* or *Kdr* (**Supplementary Fig. 6**) but strongly increased *Pdgfb* mRNA expression (**Fig. 2b**). PDGF-B is a key regulator of mural cell recruitment, serving as an attractant

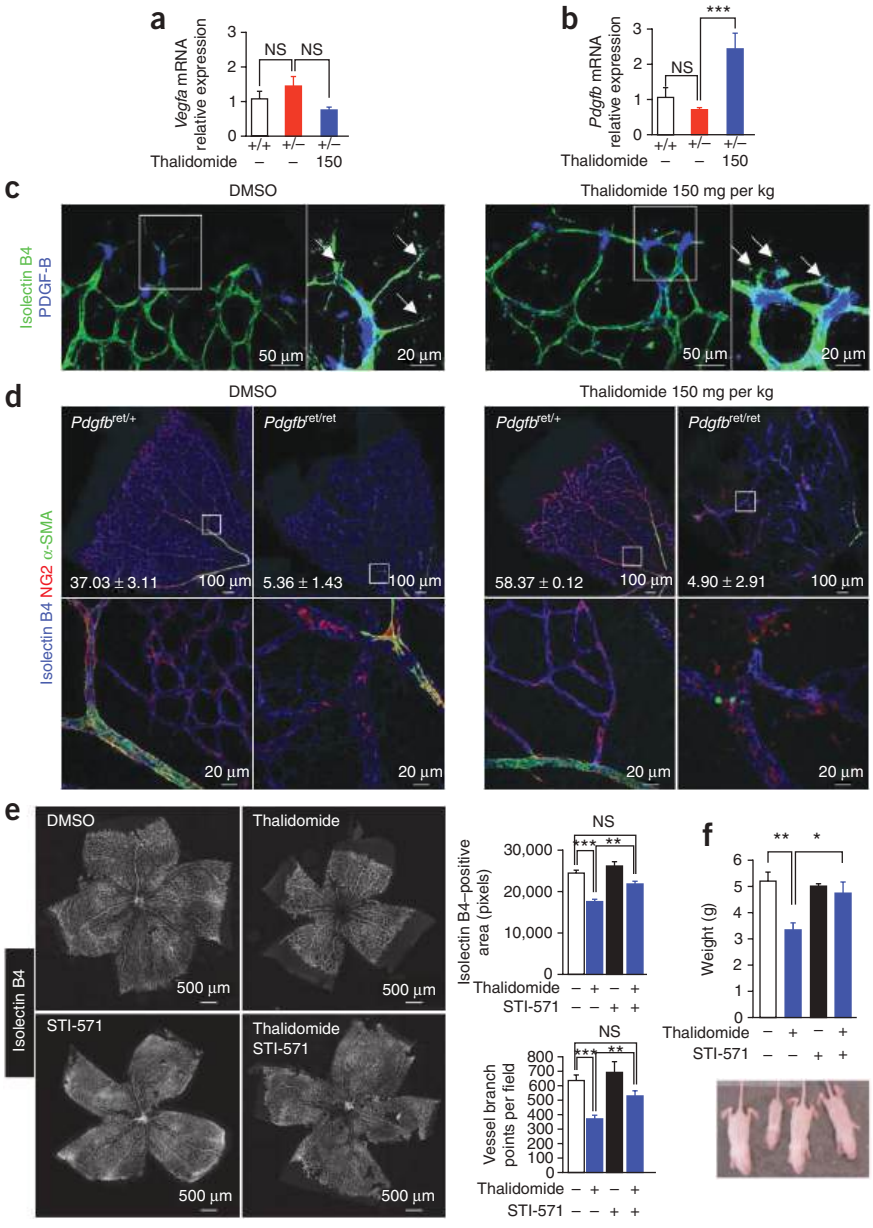

Figure 2 Thalidomide mediates vessel coverage by regulating pericyte function. (**a**) Effect of 150 mg per kg body weight thalidomide injected on P4 on *Vegfa* mRNA expression in the retina at P7, as determined by quantitative PCR. (**b**) Effect of 150 mg per kg body weight thalidomide injected on P4 on *Pdgfb* mRNA expression at P7, as determined by quantitative PCR. In **a** and **b**, $n = 6$ wild-type pups, $n = 13$ *Eng*$^{+/-}$ pups and $n = 6$ *Eng*$^{+/-}$ pups treated with thalidomide. (**c**) *In situ* hybridization for PDGF-B (blue) in combination with isolectin B4 (endothelial cell) immunostaining (green) at P7 in mice injected on P4 with DMSO (carrier control) or 150 mg per kg body weight thalidomide. Higher-magnification images of the endothelial tip cells in boxes are shown at right. Arrows in enlargements indicate characteristic cell protrusions in PDGF-B–expressing tip cells in control mice and in mice exposed to thalidomide. $n = 3$ per group. (**d**) Confocal images showing the effects of DMSO (carrier control) or thalidomide injected intraperitoneally on P4 in *Pdgfb*$^{ret/+}$ mice (in which PDGF is secreted and becomes associated with the extracellular matrix normally) and in *Pdgfb*$^{ret/ret}$ mice (in which PDGF-B does not form a gradient). Isolectin B4 staining marks endothelial cells blue, NG2 staining marks pericytes red and α-SMA staining marks vascular smooth muscle cells green. The ratio of the total area of NG2-positive pericytes (red) to that of isolectin B4–positive capillaries (blue) is indicated in each image. $n = 3$ per group. (**e**) Left, confocal imaging showing the effects of treatment on P4 with thalidomide (150 mg per kg body weight) ($n = 12$) or DMSO ($n = 10$) alone or in combination with STI-571 (50 mg per kg body weight) ($n = 10$) or with STI-571 alone ($n = 6$) on wild-type mouse retinas at P7. Isolectin-B4 staining of endothelial cells in a black-and-white image indicates the edge of the vascular front. Right, quantification of isolectin B4–positive surface area density (top) and number of vessel branch points per field (bottom). (**f**) Quantification of mouse body weight at P7 after treatment at P4 with DMSO (vehicle control), thalidomide, STI-571 or a combination of thalidomide and STI-571. The mice shown at the bottom are examples on P7 of (from left to right) control wild-type mice and mice treated on P4 with thalidomide, STI-571 or both thalidomide and STI-571. Values are given as means ± s.e.m. * $P \leq 0.05$; ** $P \leq 0.01$; *** $P \leq 0.001$.

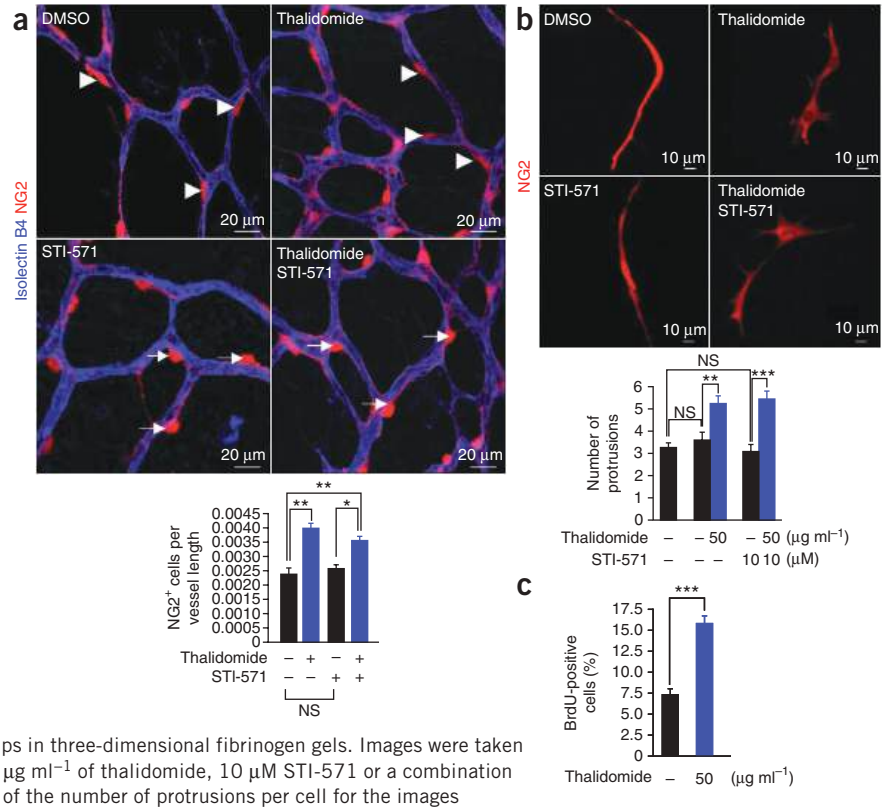

Figure 3 Effects of thalidomide on pericytes. (**a**) Top, confocal imaging showing the effects of thalidomide and inhibition of PDGF signaling by STI-571 on the association between endothelial cells of the vascular plexus, marked in blue by isolectin B4 staining, and pericytes, marked in red, in the retinas of NG2DsRedBAC-transgenic mice. Retinas were from P7 mice after intraperitoneal injection on P4 with DMSO ($n = 4$), STI-571 alone ($n = 7$), thalidomide (150 mg per kg body weight) alone ($n = 7$) or thalidomide in combination with STI-571 (50 mg per kg body weight) ($n = 8$). Dendritic processes extended by pericytes that associate intimately with the abluminal endothelial surface in both control and thalidomide-treated conditions are indicated by white arrowheads. White arrows indicate pericytes with dendritic processes partially detached from the endothelial cells in STI-571–treated pups. Bottom, quantification of the number of pericytes per isolectin-B4–stained surface area on P7 after treatment with DMSO (vehicle control), thalidomide (150 mg per kg body weight) alone, STI-571 (50 mg per kg body weight) alone or a combination of thalidomide and STI-571. (**b**) Top, confocal imaging showing the effect of STI-571 on protrusions induced by thalidomide on cultured FACS-isolated DsRed$^+$ cells from lungs of P7 NG2DsRedBAC-transgenic pups in three-dimensional fibrinogen gels. Images were taken 3 h after the addition of DMSO (vehicle control), 50 μg ml^{-1} of thalidomide, 10 μM STI-571 or a combination of thalidomide and STI-571. Bottom, quantification of the number of protrusions per cell for the images shown. Results are representative of six independent experiments. (**c**) The effect of 50 μg ml^{-1} thalidomide on BrdU labeling of FACS-isolated P7 lung DsRed$^+$ cells cultured for 3 d in presence of 0.1% FBS, epidermal growth factor and basic fibroblast growth factor. Results are representative of three independent experiments. All error bars represent s.e.m. $^*P < 0.05$, $^{**}P < 0.01$ and $^{***}P < 0.001$, results from unpaired t test.

for migrating pericytes expressing platelet-derived growth factor receptor-β (PDGFR-β)[26–29]. *In situ* hybridization showed that *Pdgfb* was expressed by endothelial tip cells and not by pericytes in both control and thalidomide-treated mice (**Fig. 2c**), indicating that thalidomide-mediated upregulation of endothelial *Pdgfb* might enhance pericyte recruitment by a paracrine mechanism.

To test this hypothesis, we took advantage of the *Pdgfb*$^{ret/ret}$ mouse model in which PDGF-B is secreted but is not retained (ret) by the extracellular matrix and so does not form the gradient required to stimulate tight adhesion of pericytes to the abluminal surface of microvessels; this lack of gradient formation leads to retinal vascular defects (**Fig. 2d**)[30]. Injection of thalidomide did not rescue the pericyte recruitment defect in postnatal *Pdgfb*$^{ret/ret}$ mice (**Fig. 2d**), supporting the idea that PDGF-B is required for thalidomide-mediated pericyte recruitment. Moreover, simultaneous treatment of postnatal wild-type mice with a high dose of thalidomide and with STI-571 (also known as imatinib mesylate or Gleevec), a potent inhibitor of PDGF receptor tyrosine kinase activity[31,32], was sufficient to restore postnatal retinal vascular development (**Fig. 2e**) and growth of pups (**Fig. 2f**). Thus, blocking PDGF signaling counteracts the effects of thalidomide on angiogenesis and on pericyte apposition to endothelial cells of the blood vessels, establishing PDGF as a key mediator of thalidomide's effects.

Thalidomide directly affects mural cell behavior

Concurrent administration of STI-571 did not inhibit the increase in the number of pericytes observed in thalidomide-treated mice (**Fig. 3a**), indicating that thalidomide may influence pericyte number directly, independently of PDGF-B. However, pericytes were only loosely associated with endothelial cells in STI-571–treated mice compared with control mice and mice treated with thalidomide alone (**Fig. 3a**). These results indicate that there may be effects on mural cells independent of PDGF-B. To test whether thalidomide indeed directly affects mural cells, we sorted DsRed$^+$ cells by FACS from lungs of P7 NG2DsRedBAC-transgenic pups and then cultured the DsRed$^+$ cells on fibrin. We confirmed the pericyte/VSMC identity of the purified DsRed$^+$ cell population by mRNA expression and staining for α-SMA, desmin and PDGFR-β (**Supplementary Fig. 7**). Treatment of these cell cultures with thalidomide for 3 h led to the formation of membrane protrusions from the cultured pericytes that became long and highly branched extensions (**Fig. 3b**). This effect was even more pronounced at 12 h (**Supplementary Fig. 8**) and was not affected by the additional presence of STI-571, indicating that the induction of membrane protrusions by thalidomide is independent of PDGF receptor signaling. These rod-like membrane protrusions resembled dendritic extensions that we suggest could function as guiding or exploratory devices.

To test whether thalidomide directly controls mural cell proliferation, we exposed cultures to BrdU for 3 h. Thalidomide-treated pericyte/VSMC cultures showed a twofold increase in the number of BrdU-labeled cells compared to DMSO (vehicle control)-treated cultures (**Fig. 3c**), providing evidence for a direct role of thalidomide as a regulator of mural cell behavior.

Thalidomide rescues vessel wall defects in *Eng*$^{+/-}$ mice

Abnormalities in the vascular wall throughout the mucosal and cutaneous vasculature are the pathological hallmark of HHT, although the number and location of lesions are highly variable and depend

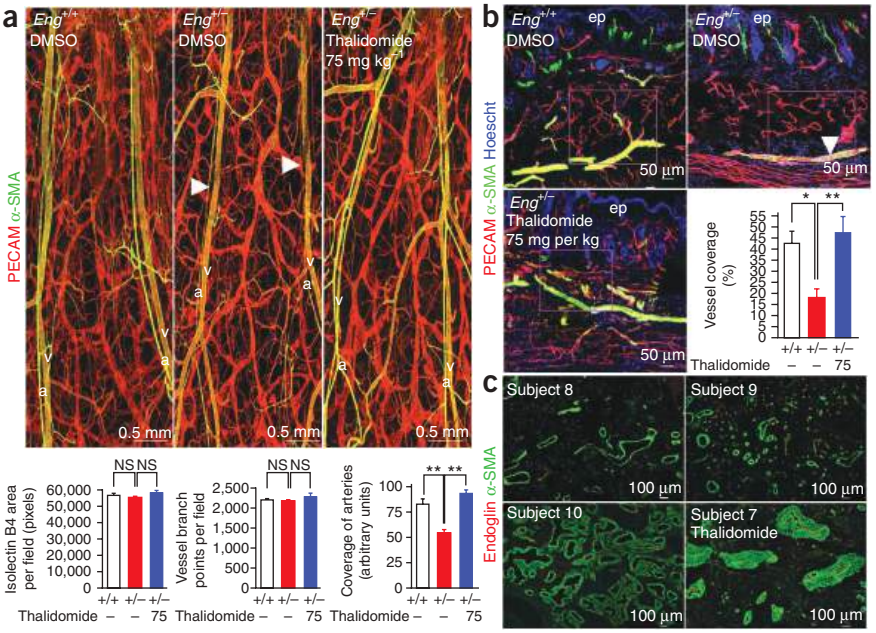

Figure 4 Thalidomide normalizes vessel coverage defects in *Eng*$^{+/-}$ mice. (**a**) Top, confocal imaging showing the effects of intraperitoneal thalidomide injection (75 mg per kg body weight) at P7 and P21 on vessel coverage in the ears of *Eng*$^{+/-}$ mice ($n = 18$) compared to DMSO-treated wild-type ($n = 9$) and *Eng*$^{+/-}$ mice ($n = 9$) at P28. On whole mounts stained for PECAM-1 (red, endothelial cells) and α-SMA (green, VSMCs), arrowheads indicate where VSMC coverage of the arteries is defective in the ears of *Eng*$^{+/-}$ mice. Bottom, quantification of PECAM-1–positive surface area density, number of vessel branches and the relative green (VSMC) intensity of the arteries measured by Metamorph software for the whole mounts shown. (**b**) Confocal images of the subcutis area of the dorsal skin stained with antibody to PECAM-1 (red) and antibody to α-SMA (green) of aged wild-type ($n = 5$) and *Eng*$^{+/-}$ ($n = 5$) mice in the absence of thalidomide and in mice treated twice weekly for 8 weeks with 75 mg per kg body weight of thalidomide ($n = 6$). The white arrowhead indicates irregular coating of the medium artery by VSMCs in the untreated *Eng*$^{+/-}$ mice. Bottom right, the effect of thalidomide injection on the ratio of total area of α-SMA–positive VSMCs to that of PECAM-positive vessels in dorsal skin of aged mice (60–70 weeks). The outlined boxes in the micrographs indicate the areas in which vessel coverage was quantified. (**c**) Confocal imaging showing the effect of daily treatment with 100 mg of thalidomide on vascular smooth muscle cell coverage of vessels in the nose in three control subjects with HHT and in one subject after daily treatment with 100 mg of thalidomide (**Table 1** and **Supplementary Fig. 1**). VSMCs are stained for α-SMA (green) and endoglin (red; endothelial cells appear as a very thin layer of flat cells). All error bars represent s.e.m. $*P < 0.05$ and $**P < 0.01$, results from unpaired *t* test. a, arteries; v, veins; ep, epidermis.

on age[4]. As in individuals with HHT, irregular layers of smooth muscle cells have been reported in the vasculature of the skin of adult *Eng*$^{+/-}$ mice; this results in fragile vessels that are prone to bleeding[22]. To test whether thalidomide could rescue this 'thin-walled vessel' aspect of the HHT phenotype, we examined vessel growth and maturation during the first postnatal month in the ear skin of *Eng*$^{+/-}$ mice. During this period, the vascular finger-like architecture of the ear expands longitudinally in a simple fashion to accommodate the growth of the tissue[33]. We stained whole mounts of 1-month-old mouse ears for PECAM-1 and α-SMA (**Fig. 4a**). This staining showed that the overall vessel morphology and patterning in *Eng*$^{+/-}$ mice was very similar to that in wild-type littermates with no differences in vessel area density or number of branch points. Veins and lymphatic vessels showed normal vessel coverage. However, arteries in the ear skin of *Eng*$^{+/-}$ mice reproducibly showed loose and irregular coverage by smooth muscle cells, although the arteries themselves were of normal size. Where present, the VSMCs were still circumferentially aligned as in wild-type mice, with the cells being perpendicular to the direction of blood flow, but large areas of the arteries failed to show normal VSMC coverage. Thalidomide administered twice at a dose of 75 mg per kg body weight, once at P7 and once at P21, was sufficient to rescue the arterial coverage defects in *Eng*$^{+/-}$ mice, resulting in a regular smooth muscle cell coating (**Fig. 4a**). Notably, neither vessel morphology and patterning nor vessel area density was affected by thalidomide treatment, suggesting that thalidomide can stimulate mural cell coverage without affecting vessel growth.

Next, we explored the effects of prolonged treatment of thalidomide in aged adult mice (60–70 weeks old), in which the vasculature is quiescent. Analysis of dorsal skin sections of *Eng*$^{+/-}$ mice stained with PECAM-1–specific and α-SMA–specific antibodies revealed widespread abnormalities in the vessel walls. We observed fewer vessels with α-SMA^{+} associated cells in the subcutis area of *Eng*$^{+/-}$ as compared to wild-type mice (**Fig. 4b**). Moreover, the arteries of *Eng*$^{+/-}$ mice were irregularly coated by VSMCs (**Fig. 4b**). Of note, thalidomide at a dose of 75 mg per kg body weight administered twice weekly for at least 2 months rescued the mural cell coverage defects of the vessels in the subcutis area, as assessed by measuring the ratio of PECAM^{+} vessels covered by α-SMA^{+} cells, although the vessel area density was unchanged (**Fig. 4b**). Moreover, in the thalidomide-treated *Eng*$^{+/-}$ mice, capillaries in the dermis, where only few α-SMA^{+} cells would normally be found, were covered by regular layers of smooth muscle cells, especially near their branch points with arterioles (**Fig. 4b**). We did not observe any long-term systemic effects of thalidomide on the vasculature, as evidenced by similarities in the density of tracheal vessels between *Eng*$^{+/-}$ mice treated for 6 months with thalidomide and untreated mice (**Supplementary Fig. 9**).

Thalidomide stimulates vessel coverage in humans

We stained sections of human nasal mucosal biopsies for endoglin and α-SMA as markers of endothelial cells and VSMCs, respectively. We compared staining in sections isolated from three untreated individuals with HHT and in sections isolated from the one individual with HHT who had received a daily 100-mg dose of thalidomide but had withdrawn for the treatment group (although this individual seemed to benefit from the treatment in terms of prevention of epistaxis, he withdrew from the study because of neuropathy) (**Fig. 4c**, **Table 1** and **Supplementary Fig. 1**). There were many more smooth muscle cell layers around the blood vessels of the treated individual (**Fig. 4c**), suggesting that mechanisms similar to those we uncovered in *Eng*$^{+/-}$ mice may be relevant to humans and may explain the clinical response to thalidomide treatment.

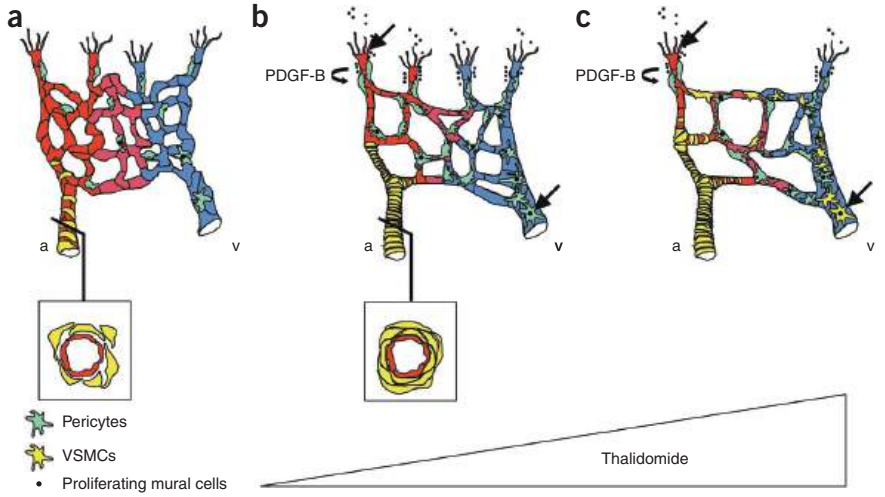

Figure 5 Schematic illustration of how thalidomide normalizes vascular malformations in HHT. (**a**) Reduced expression of endoglin or ALK-1 in endothelial cells reduces pericyte recruitment. Smooth muscle cell coverage of arteries is irregular, and vessels show endothelial hyperplasia and irregular capillary diameter. (**b**) A low dose of thalidomide normalizes vessel coverage defects and excessive angiogenesis by stimulating mural cell recruitment. Mechanisms of thalidomide-induced vessel maturation include increased PDGF-B expression from the endothelial tip cells, which attracts comigrating mural cells, and direct stimulation of mural cell proliferation. (**c**) A high dose of thalidomide enhances the number of mural cells expressing α-SMA, indicating vessel maturity, and inhibits angiogenesis. Black arrows indicate that thalidomide targets both endothelial tip cells and mural cells directly to control vessel growth and maturation. a, artery; v, vein.

DISCUSSION

Although studies conducted over the last few years have shed considerable light on cellular mechanisms underlying vascular malformations in HHT, treatment of these vascular anomalies, disseminated over entire mucosal surfaces, has remained a clinical challenge[10]. Here, we found that oral administration of thalidomide reduced both the frequency and the duration of nosebleeds and blood transfusion requirements in a small group of subjects with HHT. Hemoglobin concentrations also rose, which we infer to be a consequence of reduced hemorrhage. Moreover, we showed that the antihemorrhagic property of thalidomide is not the result of direct inhibition of endothelial cell proliferation and migration, but rather is due to increased mural cell coverage of the vasculature. We found that thalidomide modulates the activation of mural cells, increasing both their proliferation and their ability to form protrusions that embrace blood vessels. This effect on protrusion formation by inference leads to vessel stabilization. We also uncovered a key role for PDGF-B signaling in this process.

Our previous work indicated that an important consequence of defective TGF-β signaling in HHT is dysfunctional processing and activation of TGF-β by endothelial cells[8]. The availability of active TGF-β from endothelial cells is thus reduced, affecting mural cell recruitment and vessel stabilization[8]. These vascular abnormalities coincide with endothelial hyperplasia and an abnormally variable capillary diameter in the skin of *Eng*$^{+/-}$ mice[22] (**Fig. 5a**). Vessels may thus become fragile and prone to bleeding, the pathological hallmark of HHT. In the models of angiogenesis investigated here, we found that in all cases thalidomide enhanced mural cell recruitment to blood vessels (**Fig. 5b**). Mural cells are subdivided into VSMCs that surround arteries and veins in multiple concentric layers and pericytes that are either solitary or form a single, often discontinuous, layer around small-diameter blood vessels. Targeted deletions of individual components of the signaling pathways that regulate mural cell recruitment and endothelial cell–mural cell contact have previously demonstrated a crucial function of mural cells in mediating vessel stabilization[34]. Mural cells have been shown to suppress endothelial cell proliferation and migration *in vitro*[35,36] and *in vivo*[26,28], both through direct mural cell-endothelial cell contact as well as contact-independent mechanisms.

We found that excessive angiogenesis in the retinas of *Eng*$^{+/-}$ mice was normalized by administration of low doses of thalidomide, and that low and high doses of thalidomide stimulated pericyte proliferation and promoted endothelial cell–pericyte contacts (**Fig. 5b**). Apart from increasing the number of pericytes (identified by their expression of NG2, location in the retina and, at this stage and position, lack of α-SMA expression), high doses of thalidomide increased the number of pericytes in the mouse retina that expressed α-SMA, an established marker of the pericyte contractile phenotype (**Fig. 5c**). This finding correlated with an inhibition of angiogenesis and weight loss in pups treated with high doses of thalidomide; both of these effects were reversed by pharmacological inhibition of PDGF signaling, which affects endothelial cell–mural cell contact. Our results strongly suggest that the inhibitory effect of thalidomide on the excessive vasculature in the retina of *Eng*$^{+/-}$ mice is due to the increased proliferation of mural cells, their association with blood vessels in higher numbers and, possibly, the acquisition of a contractile phenotype. Indeed, pericytes share the basal lamina with endothelial cells and extend numerous cellular processes[26,28,35,36]. This interaction leads to suppression of the formation of endothelial sprouts and quiescence of the vasculature[26,28,35,36] (**Fig. 5c**).

At the molecular level, we found that thalidomide stimulated expression of PDGF-B by endothelial tip cells. Pericyte number is crucial for the normal development of a regular retinal vessel network. It has been shown, for example, that targeted deletion of PDGF-B in the endothelium results in mice that are viable but have extensive individual variation in the density of pericytes throughout the central nervous system. As consequence, these mutant mice develop a broad spectrum of vascular abnormalities in the retina, ranging from an increased number of regressing capillary branches and the presence of microaneurysms in mice with >50% of normal pericyte density, to the formation of regions of chaotic vascular organization with markedly increased vascular density in mice with <50% of normal pericyte density[29]. PDGF-B also has a crucial role in the recruitment of pericytes to newly formed vessels as well as in the remodeling of arteries, where it serves as an attractant for comigrating endothelial cells and pericytes, which express PDGFR-β. Studies in mice with endothelium-specific deletion of PDGF-B have demonstrated the key contribution of pericytes to vessel stabilization[29,30].

We found that thalidomide might also target mural cells directly to stimulate their proliferation and ability to form protrusions independently of effects on PDGF-B signaling. The exact mechanisms underlying this effect, however, need further investigation. From our *in vitro*

analysis in embryoid bodies, we cannot exclude direct targeting of newly formed vessels by thalidomide (**Fig. 5c**), as recently suggested by experiments with CSP49, an analog of thalidomide, in chick embryos. In this study, CPS49 treatment transiently blocked distal outgrowth from all vessels and, of more relevance, severely affected the survival of immature, highly angiogenic vessels (which are branches composed of stalk cells guided by tip cells) but not more mature ones, which do not have tip cells[14]. The mechanisms by which CPS49 inhibits the formation of new endothelial sprouts in immature vessels are unclear, although CPS49 has been shown to induce the stress response kinase p38α, which can promote endothelial cell death. However, our data indicate that the primary effect of thalidomide is to induce vessel maturation rather than to target endothelial sprouts. In fact, only high doses of thalidomide that reached the solubility threshold inhibited sprouting angiogenesis *in vitro*, and for all doses tested that were not lethal *in vivo*, we could counteract the inhibitory effects of thalidomide on angiogenesis by using the PDGF signaling inhibitor STI-571. We also found that thalidomide did not affect the general architecture of the vascular plexus of the ear in mice in the period during which it is still expanding to accommodate growth of the tissue, and long-term treatment with thalidomide did not affect vessel morphology or patterning or vessel area density.

Thalidomide's antiangiogenic properties have been attributed to direct effects on endothelial cells. Thalidomide has already shown activity in various experimental models of cancers[20] and is currently being investigated in early-phase clinical trials for effects on solid tumors. Our data suggest another mechanism by which thalidomide might interfere with tumor growth, namely through enhancing vessel maturation. Tumor vessels in mice lacking *Rgs5,* encoding a regulator of G-protein signaling, have recently been shown to have increased pericyte coverage, with an increased proportion of pericytes expressing α-SMA, indicating increased vessel maturation[37]. This effect on vessel maturation was associated with increased T cell infiltration of the tumor and reduced tumor size[37]. Thalidomide is also a potent immunomodulator and can enhance T cell activation[20]. Thalidomide may thus target tumor growth by enhancing both vessel maturation and T cell activation. We also speculate that the effects of thalidomide on pericytes might influence endothelial cell–leukocyte crosstalk, perhaps thereby affecting immune cell attachment to the vessel wall and their transmigration into the tumor.

For vascular abnormalities to develop, the quiescent endothelium must escape its growth-arrested state by actively destabilizing and disengaging from associated mural cells. Activation of massive local early-stage angiogenesis, commonly observed as a result of exposure to high concentrations of VEGF, is associated with vessel wall destabilization, supporting this hypothesis, which has been suggested to explain the etiology of vascular malformations[10]. Our data demonstrate that thalidomide reduces the frequency and duration of nosebleeds in subjects with HHT by stimulating vessel maturation and provide, to our knowledge, the first evidence that a therapy targeting mural cells, rather than endothelial cells, can have beneficial effects on bleeding from vascular malformations. If, as our data suggest, thalidomide or its analogs can target pericytes or mural cells, new avenues for vascular therapy may be opened up.

METHODS

Methods and any associated references are available in the online version of the paper at http://www.nature.com/naturemedicine/.

Note: Supplementary information is available on the Nature Medicine website.

ACKNOWLEDGMENTS

We thank A. Nishiyama (University of Connecticut Stem Cell Institute) for providing NG2DsRedBAC mice. This work was supported by grants from Institut National de la Santé et de la Recherche Médicale, Agence Nationale de la Recherche (Agence Nationale de la Recherche blanc, Neuroscience), Fondation pour la Recherche Médicale, Fondation Bettencourt, Association pour la Recherche sur le Cancer (3980), the Netherlands Heart Foundation (2008B106), the British Heart Foundation, the EU (QLG1-CT-2001-01032), Stichting Wetenschappelijk Onderzoek Rendu Osler and the Besluit subsidies investeringen kennisinfrastructuur program 'Dutch Platform for Tissue Engineering' and HHT Foundation International.

AUTHOR CONTRIBUTIONS

F.L. designed and performed experiments, interpreted results and wrote the paper; S.S. and S.M. performed real-time PCR, mouse retina and skin immunofluorescence experiments; K.R. performed FACS sorting and *in vitro* cell culture experiments, interpreted results and helped write the paper; C.F. and C.B. performed retina experiments; S.v.d.B. performed stem cell experiments; T.M. and B.L. performed three-dimensional fibrinogen gel culture experiments; J.-L.T. provided NG2DsRedBAC and *Pdgfb*$^{ret/+}$ mice; H.M.A. provided endoglin-knockout mice; C.J.J.W., F.D., J.J.M. and R.J.S. directed the clinical study, performed surgery, provided clinical samples and interpreted results; A.E. and C.L.M. designed experiments, interpreted results and wrote the paper.

COMPETING FINANCIAL INTERESTS

The authors declare no competing financial interests.

Published online at http://www.nature.com/naturemedicine/.
Reprints and permissions information is available online at http://npg.nature.com/reprintsandpermissions/.

1. McAllister, K.A. *et al.* Endoglin, a TGF-β binding protein of endothelial cells, is the gene for hereditary haemorrhagic telangiectasia type 1. *Nat. Genet.* **8**, 345–351 (1994).
2. Johnson, D.W. *et al.* Mutations in the activin receptor–like kinase 1 gene in hereditary haemorrhagic telangiectasia type 2. *Nat. Genet.* **13**, 189–195 (1996).
3. Lebrin, F., Deckers, M., Bertolino, P. & Ten Dijke, P. TGF-β receptor function in the endothelium. *Cardiovasc. Res.* **65**, 599–608 (2005).
4. Lebrin, F. & Mummery, C.L. Endoglin-mediated vascular remodeling: mechanisms underlying hereditary hemorrhagic telangiectasia. *Trends Cardiovasc. Med.* **18**, 25–32 (2008).
5. Govani, F.S. & Shovlin, C.L. Hereditary haemorrhagic telangiectasia: a clinical and scientific review. *Eur. J. Hum. Genet.* **17**, 860–871 (2009).
6. Cirulli, A. *et al.* Vascular endothelial growth factor serum levels are elevated in patients with hereditary hemorrhagic telangiectasia. *Acta Haematol.* **110**, 29–32 (2003).
7. Letarte, M. *et al.* Reduced endothelial secretion and plasma levels of transforming growth factor-β1 in patients with hereditary hemorrhagic telangiectasia type 1. *Cardiovasc. Res.* **68**, 155–164 (2005).
8. Carvalho, R.L. *et al.* Defective paracrine signalling by TGFβ in yolk sac vasculature of endoglin mutant mice: a paradigm for hereditary haemorrhagic telangiectasia. *Development* **131**, 6237–6247 (2004).
9. ten Dijke, P. & Arthur, H.M. Extracellular control of TGFβ signalling in vascular development and disease. *Nat. Rev. Mol. Cell Biol.* **8**, 857–869 (2007).
10. Bauditz, J. & Lochs, H. Angiogenesis and vascular malformations: antiangiogenic drugs for treatment of gastrointestinal bleeding. *World J. Gastroenterol.* **13**, 5979–5984 (2007).
11. Kabbinavar, F. *et al.* Phase II, randomized trial comparing bevacizumab plus fluorouracil (FU)/leucovorin (LV) with FU/LV alone in patients with metastatic colorectal cancer. *J. Clin. Oncol.* **21**, 60–65 (2003).
12. Bose, P., Holter, J.L. & Selby, G.B. Bevacizumab in hereditary hemorrhagic telangiectasia. *N. Engl. J. Med.* **360**, 2143–2144 (2009).
13. D'Amato, R.J., Loughnan, M.S., Flynn, E. & Folkman, J. Thalidomide is an inhibitor of angiogenesis. *Proc. Natl. Acad. Sci. USA* **91**, 4082–4085 (1994).
14. Therapontos, C., Erskine, L., Gardner, E.R., Figg, W.D. & Vargesson, N. Thalidomide induces limb defects by preventing angiogenic outgrowth during early limb formation. *Proc. Natl. Acad. Sci. USA* **106**, 8573–8578 (2009).
15. Bauditz, J., Schachschal, G., Wedel, S. & Lochs, H. Thalidomide for treatment of severe intestinal bleeding. *Gut* **53**, 609–612 (2004).
16. Dabak, V., Kuriakose, P., Kamboj, G. & Shurafa, M. A pilot study of thalidomide in recurrent GI bleeding due to angiodysplasias. *Dig. Dis. Sci.* **53**, 1632–1635 (2008).
17. Kamalaporn, P. *et al.* Thalidomide for the treatment of chronic gastrointestinal bleeding from angiodysplasias: a case series. *Eur. J. Gastroenterol. Hepatol.* **21**, 1347–1350 (2009).
18. Kurstin, R. Using thalidomide in a patient with epithelioid leiomyosarcoma and Osler-Weber-Rendu disease. *Oncology* (Williston Park) **16**, 21–24 (2002).

19. Pérez-Encinas, M., Rabunal Martinez, M.J. & Bello Lopez, J.L. Is thalidomide effective for the treatment of gastrointestinal bleeding in hereditary hemorrhagic telangiectasia? *Haematologica* **87**, ELT34 (2002).
20. Melchert, M. & List, A. The thalidomide saga. *Int. J. Biochem. Cell Biol.* **39**, 1489–1499 (2007).
21. Jakobsson, L., Kreuger, J. & Claesson-Welsh, L. Building blood vessels-stem cell models in vascular biology. *J. Cell Biol.* **177**, 751–755 (2007).
22. Torsney, E. *et al.* Mouse model for hereditary hemorrhagic telangiectasia has a generalized vascular abnormality. *Circulation* **107**, 1653–1657 (2003).
23. Bourdeau, A., Dumont, D.J. & Letarte, M. A murine model of hereditary hemorrhagic telangiectasia. *J. Clin. Invest.* **104**, 1343–1351 (1999).
24. Fruttiger, M. Development of the retinal vasculature. *Angiogenesis* **10**, 77–88 (2007).
25. Zhu, X., Bergles, D.E. & Nishiyama, A. NG2 cells generate both oligodendrocytes and gray matter astrocytes. *Development* **135**, 145–157 (2008).
26. Lindahl, P., Johansson, B.R., Leveen, P. & Betsholtz, C. Pericyte loss and microaneurysm formation in PDGF-B–deficient mice. *Science* **277**, 242–245 (1997).
27. Hellström, M., Kalen, M., Lindahl, P., Abramsson, A. & Betsholtz, C. Role of PDGF-B and PDGFR-β in recruitment of vascular smooth muscle cells and pericytes during embryonic blood vessel formation in the mouse. *Development* **126**, 3047–3055 (1999).
28. Hellström, M. *et al.* Lack of pericytes leads to endothelial hyperplasia and abnormal vascular morphogenesis. *J. Cell Biol.* **153**, 543–553 (2001).
29. Enge, M. *et al.* Endothelium-specific platelet-derived growth factor-B ablation mimics diabetic retinopathy. *EMBO J.* **21**, 4307–4316 (2002).
30. Lindblom, P. *et al.* Endothelial PDGF-B retention is required for proper investment of pericytes in the microvessel wall. *Genes Dev.* **17**, 1835–1840 (2003).
31. Dudley, A. *et al.* STI-571 inhibits *in vitro* angiogenesis. *Biochem. Biophys. Res. Commun.* **310**, 135–142 (2003).
32. Hasumi, Y. *et al.* Identification of a subset of pericytes that respond to combination therapy targeting PDGF and VEGF signaling. *Int. J. Cancer* **121**, 2606–2614 (2007).
33. Vollmar, B., Morgenthaler, M., Amon, M. & Menger, M.D. Skin microvascular adaptations during maturation and aging of hairless mice. *Am. J. Physiol. Heart Circ. Physiol.* **279**, H1591–H1599 (2000).
34. Gaengel, K., Genove, G., Armulik, A. & Betsholtz, C. Endothelial-mural cell signaling in vascular development and angiogenesis. *Arterioscler. Thromb. Vasc. Biol.* **29**, 630–638 (2009).
35. Orlidge, A. & D'Amore, P.A. Inhibition of capillary endothelial cell growth by pericytes and smooth muscle cells. *J. Cell Biol.* **105**, 1455–1462 (1987).
36. Sato, Y. & Rifkin, D.B. Inhibition of endothelial cell movement by pericytes and smooth muscle cells: activation of a latent transforming growth factor-β 1–like molecule by plasmin during co-culture. *J. Cell Biol.* **109**, 309–315 (1989).
37. Hamzah, J. *et al.* Vascular normalization in Rgs5-deficient tumours promotes immune destruction. *Nature* **453**, 410–414 (2008).

ONLINE METHODS

Subjects and nasal biopsies. Clinical studies were approved by the Medical Ethics Committee of the St. Antonius Hospital, where we recruited the subjects, who provided informed consent. This investigation conforms to the principles of the Declaration of Helsinki. We collected nose biopsies in physiological salt, fixed them overnight in 0.2% paraformaldehyde in 0.1 M phosphate buffer with 0.12 mM $CaCl_2$ and 4% sucrose and then processed them as previously described[38]. We used 10-μm sections for staining.

Thalidomide and immunoreagents. Suppliers and manufacturers are given in the **Supplementary Methods**.

Mice and tissues. We maintained *Eng*$^{+/-}$, NG2DsRedBAC and *Pdgfb*$^{ret/+}$ mice[25,30,39] as heterozygotes on a mixed C57BL/6 and CBA genetic background. The Animal Experiments Committee of Ile de France approved all protocols. We injected thalidomide and STI-571 intraperitoneally (volume 20 μl). Control mice received vehicle only.

To analyze postnatal angiogenesis in the mouse retina, we injected pups once at P4 with 50–150 mg per kg body weight of thalidomide, 50 mg per kg body weight of STI-571 or both and killed them at P7. We fixed their eyes in 4% paraformaldehyde in PBS at 20 °C for 10 min, dissected the retinas, post-fixed them in 4% paraformaldehyde in PBS at 4 °C overnight and then processed them for immunostaining.

For whole-mount analysis of cutaneous blood vessels, we treated mice at P7 and P21 with 75 mg per kg body weight of thalidomide, killed them at P30 and dissected the ears with forceps, separating the dorsal and ventral leaflets. We fixed dorsal halves in 4% paraformaldehyde overnight at 4 °C and processed them as previously described[40].

For immunofluorescent staining of dorsal skin, we injected 60-week-old mice twice weekly with 75 mg per kg body weight of thalidomide for 6 weeks. After we killed the mice, we processed dorsal skin tissues and stained 50-μm sagittal sections as previously described[38].

Immunofluorescence and immunohistochemistry. We fixed frozen sections of mouse dorsal skin or nose biopsies from subjects with HHT in cold acetone, washed them with PBS, blocked them with blocking reagent (Roche) and incubated them overnight at 4 °C with primary antibodies (**Supplementary Methods**) in PBS plus 0.2% BSA (A4503, Sigma). After washing, we incubated sections for 1 h at 20 °C with secondary antibodies diluted in PBS with 0.2% BSA and mounted them in DAKO mounting medium (S3023, DAKO). We captured images with a confocal laser-scanning microscope SP5 (Leica) or with a DMLB microscope (Leica).

We performed whole-mount immunohistochemistry of retinas as previously described[41].

Morphometry and quantitative analysis. We quantified branch points and vessel length per field as previously described[42]. We measured the total cellular area (pixels) by converting compressed Z-stacks to black and white followed by manual threshold adjustment to highlight cell contours. We quantified the cell surface area with ImageJ software (US National Institutes of Health) and counted the number of protrusions per cell (200 cells analyzed per thalidomide-treated and vehicle control group in four independent experiments).

We determined colocalization of mural cell markers with vessels on similar images with a uniform threshold between experiments and analyzed the data with the colocalization function of ImageJ to identify pixels that had fluorescence intensity in both mural cell (NG2 or α-SMA) and endothelial cell (isolectin B4 or PECAM-1) marker channels equal to or greater than a set threshold value. We measured colocalization as the overlapping pixel area and expressed it as a percentage.

We quantified α-SMA staining intensity with Metamorph 6.1 software (Universal Imaging). We set images at threshold intensity; values below this threshold were excluded from analysis. For each image of the whole ear, we delineated the vessels analyzed and calculated α-SMA intensity with the integrated intensity defined as the sum of all pixels in the delineated box.

Quantitative PCR analysis. We isolated RNA from P7 retinas and, using standard procedures (**Supplementary Methods**), analyzed expression of mouse *Acta1*, *Vegfa*, *Pdgfb*, *Flt1* and *Kdr*, normalized to a reference pool including *Pecam* and *Actb*. We performed two separate *in vitro* transcription reactions for every RNA sample. We analyzed the contralateral retinas by α-SMA, NG2 and isolectin B4 staining.

Cell sorting and three-dimensional fibrinogen gel culture. We isolated live DsRed$^+$ cells by FACS-Vantage Flow cytometer (BD) from the lungs of P7 DsRedNG2BAC-transgenic mice. We minced the lungs, digested them with 0.2 mg ml^{-1} collagenase (17100-017, Invitrogen), cultured them overnight in DMEM supplemented with 20% FBS and then sorted them. After sorting, we cultured DsRed$^+$ cells on fibrinogen gel (F4753, Sigma) with 20% FBS and DMSO, 50 μg ml^{-1} of thalidomide, 10 μM STI-571 or thalidomide and STI-571 together. We captured images at 0 h and 12 h by SP5 confocal microscopy (Leica).

Cell proliferation. We determined the effect of 50 μg ml^{-1} thalidomide on the proliferation of DsRed$^+$ cells cultured in 0.1% FBS, epidermal growth factor and basic fibroblast growth factor by BrdU incorporation (**Supplementary Methods**).

Statistical analyses. We performed statistical analyses with Prism 4 software (GraphPad) using the two-tailed, unpaired Student's *t* test. We also used the Mann-Whitney *U* test to compare the number of epistaxis in individuals with HHT before and during thalidomide treatment, for small groups of samples for which the distribution of values was unknown. We compared medians of hemoglobin concentrations (before, during and after thalidomide) for each subject with the Kruskal-Wallis test. P values < 0.05 were considered statistically significant.

Additional methods. Detailed methodology is described in the **Supplementary Methods**.

38. Bajanca, F., Luz, M., Duxson, M.J. & Thorsteinsdottir, S. Integrins in the mouse myotome: developmental changes and differences between the epaxial and hypaxial lineage. *Dev. Dyn.* **231**, 402–415 (2004).
39. Arthur, H.M. *et al.* Endoglin, an ancillary TGFβ receptor, is required for extraembryonic angiogenesis and plays a key role in heart development. *Dev. Biol.* **217**, 42–53 (2000).
40. Uutela, M. *et al.* PDGF-D induces macrophage recruitment, increased interstitial pressure, and blood vessel maturation during angiogenesis. *Blood* **104**, 3198–3204 (2004).
41. Gerhardt, H. *et al.* VEGF guides angiogenic sprouting utilizing endothelial tip cell filopodia. *J. Cell Biol.* **161**, 1163–1177 (2003).
42. Hellström, M. *et al.* Dll4 signalling through Notch1 regulates formation of tip cells during angiogenesis. *Nature* **445**, 776–780 (2007).

doi:10.1038/nm.2131